The Astrophysical Journal, 801:61 (15pp), 2015 March 1 doi:10.1088/0004-637X/801/1/61

CORRECTING THE RECORD ON THE ANALYSIS OF *IBEX* AND *STEREO* DATA REGARDING VARIATIONS IN THE NEUTRAL INTERSTELLAR WIND

P. C. Frisch[1], M. Bzowski[2], C. Drews[3], T. Leonard[4], G. Livadiotis[5], D. J. McComas[5,6], E. Möbius[4], N. Schwadron[4], and J. M. Sokół[2]
[1] Department Astronomy and Astrophysics, University of Chicago, Chicago, IL 60637, USA
[2] Space Research Centre of the Polish Academy of Sciences, Warsaw, Poland
[3] Institute for Experimental and Applied Physics, Christian-Albrechts-University zu Kiel, Germany
[4] Space Science Center, University of New Hampshire, Durham, NH 03824, USA
[5] Southwest Research Institute, San Antonio, TX 78249, USA
Received 2014 June 29; accepted 2014 December 29; published 2015 March 4

ABSTRACT

The journey of the Sun through space carries the solar system through a dynamic interstellar environment that is presently characterized by a Mach ∼1 motion between the heliosphere and the surrounding warm partially ionized interstellar cloud. The interaction between the heliosphere and interstellar medium is an evolving process due to variable solar wind properties and the turbulent nature of the interstellar cloud that surrounds the heliosphere. Frisch et al. presented a meta-analysis of the historical data on the interstellar wind flowing through the heliosphere and concluded that temporal changes in the ecliptic longitude of the flow direction with time were statistically indicated by the data available in the refereed literature at the time of that writing. Lallement & Bertaux disagree with this result, and suggested, for instance, that a key instrumental response function of *IBEX*-Lo was incorrect and that the *STEREO* pickup ion data are unsuitable for diagnosing the flow of interstellar neutrals through the heliosphere. In this paper we first show that temporal variations in the interstellar wind through the heliosphere are consistent with our knowledge of the very local interstellar medium. The statistical analysis of the helium wind data is revisited, and a recent correction of a typographical error in the literature is incorporated into the new fits. With this correction, and including no newer *IBEX* results, these combined data still indicate that a change in the longitude of the interstellar neutral wind of $\lambda = 5\overset{\circ}{.}6 \pm 2\overset{\circ}{.}4$ over the past forty years remains statistically likely, but an constant flow longitude is now statistically possible. Other scenarios for the selection of subsets of these data used in the fitting process produce similar conclusions. We show that the speculations made by Lallement & Bertin about the *IBEX* instrumental response function are incorrect, and that their other objections to the data used in the meta-analysis are either incorrect or unproven. Further investigations of the historical interstellar wind data and continuing analysis of additional *IBEX* data may provide a more definitive result on the stability of the flow of interstellar gas through the heliosphere.

Key words: ISM: structure – methods: data analysis – shock waves – solar wind – space vehicles: instruments – turbulence

1. INTRODUCTION

The solar system is traveling through a dynamically evolving interstellar medium that leads to variations in the interstellar wind through the solar system over geologically short timescales (Frisch et al. 2011; Frisch & Mueller 2011). The Local Interstellar Cloud (LIC) now around the heliosphere is a low-density and partially ionized cloud (Slavin & Frisch 2008). The relative motions of the Sun and LIC creates a wind of interstellar gas and dust through the heliosphere whose velocity was first defined by measurements of the fluorescence of solar 584 Å photons off of interstellar He^{o} in the gravitational focusing cone downwind of the Sun (Weller & Meier 1974). The absence of interstellar H^{o} at the LIC velocity toward the two nearby stars α Cen (1.3 pc) and 36 Oph (6.0 pc) indicate that the Sun will emerge from the LIC in the upwind[7] direction anytime within the next 3500 years (Lallement et al. 1995; Wood et al. 2000), and that it entered the LIC during the past 10,000 years (Frisch 1994). Variations in the interstellar wind direction over historical timescales, of about 40 years for the space age, suggest that interstellar neutrals (ISNs), and the pickup ions (PUIs) that form from them after ionization, provide the best diagnostics of the longitude of the interstellar wind flowing through the heliosphere. The dynamic characteristics of the surrounding LIC suggest that short-term variations in the interstellar wind direction may exist.

In the paper titled "Decades-Long Changes of the Interstellar Wind Through Our Solar System," Frisch et al. (2013, hereafter Paper I) have presented a meta-analysis of historical observations of the interstellar He^{o} wind data and found that the data indicated a statistically likely shift in the wind longitude of $\sim 6\overset{\circ}{.}8$ over the past forty years, and that a constant flow longitude is statistically unlikely. The historical data set included in situ measurements of the helium wind by *IBEX* (McComas et al. 2012; Möbius et al. 2012; Bzowski et al. 2012) and *Ulysses* (Witte 2004), measurements of PUIs in the downwind gravitational focusing cone by the *ACE*-SWICS, *STEREO*-PLASTIC, and *MESSENGER*-FIPS (Gloeckler et al. 2004; Drews et al. 2012; Gershman et al. 2013), the upwind crescent by *STEREO*-PLASTIC (Drews et al. 2012), and measurements of the backscattered radiation from solar He^{o} 584 Å emissions fluorescing from interstellar He^{o} in the inner

[6] Also at University of Texas in San Antonio, San Antonio, TX 78249, USA.
[7] The terms "upwind" and "downwind" refer to the direction of the heliosphere nose, which in turn is defined by the direction of the interstellar He^{o} wind that flows into the inner heliosphere.

heliosphere (Weller & Meier 1974, 1981; Ajello 1978; Ajello et al. 1979; Dalaudier et al. 1984; Vallerga et al. 2004; Nakagawa et al. 2008). This was the first meta-analysis that searched for possible historical variations in the direction of the wind of heavy ISN atoms through the heliosphere.

The original study in Paper I was restricted to heavy atoms and did not include longitude information from the velocity vectors of either interstellar H^o or interstellar dust grains flowing through the heliosphere. Both sets of particles are strongly filtered on a time-variable basis, because of the solar magnetic activity cycle, throughout the heliosphere and heliosheath regions (Ripken & Fahr 1983; Rucinski & Bzowski 1996; Saul et al. 2013; Grogan et al. 1996; Landgraf 2000; Slavin et al. 2012; Sterken et al. 2012; Strub et al. 2014).

In a paper "On the Decades-Long Stability of the Interstellar Wind through the Solar System," Lallement & Bertaux (2014, hereafter LB14) disagree with the conclusions in Paper I. The different viewpoints presented in Paper I and LB14 fall into two categories, the most interesting of which is the underlying science question that is encapsulated by the differences of the two titles On the "Decades-Long Changes of the Interstellar Wind Through Our Solar System" compared to "Decades-Long Stability of the Interstellar Wind through the Solar System." The second area of disagreement centers on the selection of data used in the analysis, and the *IBEX* instrumental parameters. LB14 favor the interstellar He^o flow direction determined in Möbius et al. (2004), where measurements of the interstellar He^o wind found by *Ulysses*, *ACE*, *EUVE*, and Prognoz 6 were combined to find the best-fitting direction for the interstellar wind. The groundwork for understanding the interstellar helium wind is presented in the set of papers that accompany Möbius et al. (2004).[8]

In this paper we first revisit the conclusions of Paper I, with the proviso that new data on, and better modeling of, the interstellar wind are creating a rapidly changing scientific data base upon which our conclusions rely. Data showing that the interstellar wind *could* change over historical times are discussed, and these data are consistent with inhomogeneities in the LIC over spatial scales comparable to the heliosphere dimensions (Section 2). New statistical analyses are performed on the historical data (Section 3), utilizing a new published correction for the uncertainties on the NOZOMI interstellar He^o wind direction (Section 4.3.3). A temporal change in the wind longitude is found to be statistically likely, but a constant wind direction also becomes statistically acceptable although less likely than a variable direction. LB14 objected to the use of the *IBEX*-Lo data in recovering a longitude for the He^o flow that differed from the value found by *Ulysses*. Methods for retrieving the flow longitude from *IBEX*-Lo data are discussed in Section 4.1, with further details on the instrumental response function and properties in Section 4.1.3 and Appendix B. Cloud temperature plays an important role in the uncertainties of the parameter space constrained by the *IBEX*-Lo data; the interstellar picture of the LIC temperature is discussed in Appendix A. The LB14 comments on the *STEREO* data are discussed in Section 4.2, where new data are mentioned that contradict the hypothesis of significant azimuthal transport of PUIs inside of 1 AU, and in Appendix C. Table 1 summarizes the data issues.

[8] The wind direction in this study needs to be corrected by 0.°7 to account for an unrecognized difference in coordinate epochs of the contributing data (Frisch et al. 2009; Lallement et al. 2010).

2. POSSIBLE SPATIAL INHOMOGENEITIES IN LIC

2.1. Turbulence and Edge Effects

The Sun moves through the surrounding interstellar cloud at a relative velocity of ∼5 AU yr^{-1}, so that the forty-year historical record of the interstellar wind velocity sampled interstellar scale lengths of ∼200 AU. There is no ad hoc reason that the LIC should be homogeneous and isotropic over such small spatial scales. The mean free path of a thermal population of LIC atoms is ∼330 AU,[9] which is larger than the distance traveled through the LIC during the past 40 years. Collisional coupling between atoms will break down over scales smaller than the mean free path, allowing the formation of eddies that perturb the gas velocity over heliosphere scale-lengths. Paper I suggested that a shift in the He^o flow direction could be due to the nonthermal turbulence of eddy motions.

A second source of small-scale turbulence in the LIC is Alfvenic turbulence. The LIC interstellar magnetic field (ISMF; McComas et al. 2009; Funsten et al. 2013) affects clumping of the charged particles over scales smaller than the collisional mean free path. The LIC magnetic field strength is ∼3 μG, based on the plasma pressure of energetic neutral atoms (ENAs) in the upwind direction and the magnetic distortion of the heliotail (Schwadron et al. 2011), and the equipartition of energy between magnetic and thermal energies in the LIC (Slavin & Frisch 2008). For field strengths of 3 μG and larger, the Lorentz force will couple protons tightly to the ISMF, over ∼375 km scales for a gas temperature of 7000 K. This tight coupling acts as a conduit for magnetic turbulence into the LIC that affects the neutral population observed by *IBEX* through charge exchange, and would perturb the neutral particle velocities over spatial scales smaller than the collisional scale.

The location of the LIC in a decelerating group of clouds that appears to be a fragment of the Loop I superbubble shell (Frisch et al. 2011) would promote turbulence in the local ISMF. If the surrounding decelerating flow of ISM (Frisch et al. 2002, 2011) consists of clouds in contact with each other, then macro-turbulence may form in the LIC at the acoustic velocity of about 8 km s^{-1}. The angle between the LIC ISMF and the flow of LIC gas through the local standard rest (LSR) is $86^\circ \pm 14^\circ$, indicating that the velocity and magnetic field vectors are perpendicular (Frisch & Schwadron 2014). Depending on the relative thermal and magnetic pressures, compressive turbulence may form. Magnetic turbulence may propagate along the bridge of polarized dust that extends from near the Sun out to the North Polar Spur region (Frisch et al. 2014). Magnetic disturbances will propagate along the ISMF at the Alfven speed of ∼25 km s^{-1} (using an electron density of 0.07 cm^{-3}, Slavin & Frisch 2008), organizing additional disruption of particle velocities over scale sizes smaller than the mean free path.

It is important to note that the thermal distribution of the He^o atoms smooths the time-interval sampled by the population observed at 1 AU because of the different propagation times of fast and slow atoms through the heliosphere. A Maxwellian gas at 7000 K has a Doppler width of ∼5 km s^{-1}, which is a significant percentage of the bulk LIC motion, causing faster particles to catch up to slower particles in the incoming He^o flow. The Maxwellian distribution will not apply over microscales less than the 330 AU mean free path of charge-exchange, and in principle the mean free paths of the higher energy atoms will be larger than 330 AU anyway.

[9] The mean free path in the LIC is dominated by charge-exchange and induced dipole scattering between H^o and H$^+$ atoms (Spangler et al. 2011).

Table 1
Comments on Lallement & Bertaux (2014) Criticisms of Data and Usage in Paper I[a]

	Argument	Comment	Section (Appendix)
Criticisms regarding IBEX analysis			
1	*Ulysses* and *IBEX* velocity–longitude combinations give same perihelion	True for hot models using Maxwellian distributions, but irrelevant to results	4.1.1 4.1.2 (B)
2	*IBEX*-Lo instrumental response correction (IRC) is wrong	Incorrect; the IRC, dead-time correction, and data throughput are well understood	4.1.3 (B)
3	Correct IRC makes *IBEX* and *Ulysses* longitudes agree	Incorrect; the *IBEX* results rely on variations of the peak as a function of latitude and observer longitude	4.1.1
4	Warsaw modeling based on wrong IRC corrections	Incorrect; Warsaw models compared to data based on a correct and tested IRC	4.1.3
Criticisms regarding STEREO analysis			
5	Short-term electron-impact ionization (EII) not included in data analysis	Incorrect; short-term EII is distinguished from long-term ionizations in methodology	4.2, 4.2.2
6	Orbit groupings are not statistically independent	Incorrect; each orbit pairing selects invariant distributions from comparisons of data acquired over separate time-spans	4.2 (C)
7	Simulations of uncertainties of *STEREO* data are incorrect	Uncertainty simulations are appropriate for variable PUI data	4.2 (C)
8	Secondary oxygen invalidates usage of oxygen PUIs	Incorrect; secondary oxygen population minor compared to primary population, and if included push longitudes into the opposite direction than suggested	4.2.3
9	Longitudes from PUI focusing cone and upwind crescent are upper limits due to transport effects inside 1 AU	Maybe, but transport effects appear to be insignificant, based on comparisons between several different data sets	4.2.1
Criticisms regarding use of Ultraviolet Data			
10	Mariner 10 longitude is based on both H^o and He^o	Incorrect: Mariner 10 papers quote longitude of He^o wind separately	4.3.1
11	He^o flow direction from Prognoz 6 geometric analysis not valid	The Prognoz 6 He^o direction from geometric arguments has uncertainties and was included since it was not repudiated in the literature	4.3.2
12	NOZOMI uncertainties of $\pm 3.^\circ 4$ are too small	True; the results of the 2014 NOZOMI erratum are used in this paper	4.3.3

Note. [a] Numbers in last column show section or appendix where the topic is discussed.

Upper limits on an interstellar Lyα component at the LIC velocity toward 36 Oph, in the upwind direction, show that the Sun is near the LIC edge (Wood et al. 2000). The high level of LIC ionization that is inferred from photoionization models requires that 22%, 39%, 0.80%, and 19% of the hydrogen, helium, neon, and oxygen atoms at the heliosphere boundaries are ionized (Slavin & Frisch 2008, SF08). A thin conductive interface between the warm LIC and hot plasma of the Local Bubble maintains these ionization levels (SF08). A sharp density decrease and velocity increase is expected at the edge between the LIC and conductive interface. The unknown distance to the upwind edge of the LIC allows that such an interface is close to the heliosphere. However, no direct observational evidence of this interface is yet found.

2.2. Supersonic Collisions between Clouds

Disturbances due to the propagation of shocks through the cloud are also possible sources of kinematical structure in the LIC. The LIC belongs to a decelerating flow of ISM through space that may create dynamical interfaces in the interaction regions between clouds in physical contact (Frisch et al. 2011). If the LIC is in physical contact with either the Blue Cloud (BC) in the downwind direction, or the G-Cloud (GC) in the upwind direction,[10] the shocks that form at the supersonic interfaces will drive compressional disturbances into the LIC that perturb the density and velocity of the gas particles.

A supersonic interface would form between the LIC and GC if they are in contact. The angle between the LIC and GC LSR velocity vectors is $17.^\circ 2$, and the relative velocity is 14.6 km s^{-1}. The G-cloud has a temperature of 5500 ± 400 K (Redfield & Linsky 2008), corresponding to an acoustic velocity of $\sim$7.7 km s^{-1}, indicating a shock strength of Mach $\sim$1.9 between the clouds.[11]

A supersonic interface would also form between the LIC and the BC if they are in contact. These clouds have LSR velocities of 15.3 ± 2.5 km s^{-1} and 7.1 ± 2.3 km s^{-1} respectively, and

[10] An independent sorting of local interstellar velocity absorption components into clouds is provided by Redfield & Linsky (2008) and we use that cloud-naming scheme here.

[11] Using instead the heliocentric velocities for the LIC and GC in the upwind direction, and now-obsolete physical parameters for both clouds, Grzedzielski & Lallement (1996) have predicted that a supersonic interface is present between the LIC and the G-cloud, with the LIC corresponding to the post-shock gas because it is warmer than the G-cloud. Frisch & York (1991) also modeled the local shock structure.

Table 2
Fits to Historical Interstellar Wind Data

Num.	Basis of Fit	Fit[a] λ(deg.)	Reduced χ^2	p-value
		A. Paper I:[b]		
1	Linear	$70.6(\pm1.6) + 0.17(\pm0.06) * t_{1970}$	0.97	0.49
2	Constant λ	$75.1(\pm1.3)$	1.71	0.031
		B. Corrected NOZOMI uncertainties:[c]		
3	Linear	$71.3(\pm1.6) + 0.14(\pm0.06) * t_{1970}$	0.7[d]	0.82
4	Constant λ	$75.0(\pm0.3)$	1.1	0.35
		C. Two *IBEX* data points, modified 584 Å uncertainties:[e]		
5	Linear	$71.4(\pm1.6) + 0.14(\pm0.06) * t_{1970}$	0.8	0.3
6	Constant λ	75.0 ± 0.3	1.3	0.2
7	Parabolic λ fit	$74.1(\pm1.4) - 0.11(\pm0.11) * t_{1970} + 5.0(\pm2.1)10^{-3} * t_{1970}^2$	0.6	0.14

Notes.
[a] λ is the ecliptic longitude of the interstellar wind and t_{1970} is the elapsed time since 1970. A p-value larger than 0.05 passes the p test and therefore is not unlikely.
[b] This fit is the original linear fit in Paper I that used the NOZOMI value from Nakagawa et al. (2008).
[c] These fits used the historical wind data in Paper I, except that the uncertainties for the NOZOMI value are corrected to incorporate the erratum of Nakagawa et al. (2014). This linear fit should replace the fit listed in Paper I. See Section 4.3.
[d] This fit is accepted and is more likely than fit number 4. The small value of χ^2 suggests that the uncertainties may be overestimated by ∼20%.
[e] These fits incorporate uncertainties for the wind longitude for the STP2-1, Mariner 10, and SOLRAD11B data that include only the longitude uncertainties (see Section 4.3). The geometric Prognoz 6 direction is omitted from the fit according to the discussion in Section 4.3. The He^o wind directions from the individual *IBEX* 2009 and 2010 observing seasons are included independently (Sections 4.1.2, 3, and see Bzowski et al. 2012).

an angle between the two vectors of 49° (cloud LSR velocities are from Frisch & Schwadron 2014). The LIC sound velocity is 8.6 km s^{-1}, for a 7000 K perfect gas with mean molecular weight 1.29. The ∼11.9 km s^{-1} relative velocity indicates a supersonic interface of Mach number ∼1.4 between the two clouds if they are in direct contact. The LIC is warmer than the BC, which has a temperature 3000^{+2000}_{-1000} K (Hebrard et al. 1999). A simple temperature gradient between the three clouds does not exist. In the presence of the ISMF, the shock transitions will be modified by the unknown angle between the magnetic field and the normal to the cloud surface.

3. REFITTING THE HISTORICAL DATA ON THE INTERSTELLAR WIND LONGITUDE

A new statistical interpretation of the historical data (Table 1 in the online supplementary material, OSM, of Paper I) is required by a typographical error in the original NOZOMI publication (Nakagawa et al. 2008). We first perform new fits to the same set of data used in the Paper I using the corrected uncertainty for the He^o flow longitude determined from the NOZOMI data (Nakagawa et al. 2014, Section 4.3.3), and next for an alternate selection of the fitted data.

The results of the refitting are presented in Table 2. The first result, heading A, shows the original fit from Paper I. The updated fit using the corrected NOZOMI uncertainties is listed under heading B, fits 3 and 4, of Table 2, and plotted in Figure 1. The slope of the revised fit is 0.14 ± 0.06, which implies a directional change of $\delta\lambda = 5.^\circ6 \pm 2.^\circ4$ over the past 40 years (instead of the $6.^\circ8 \pm 2.^\circ4$ in Paper I). The reduced χ^2 of the fit is 0.7, and the p-value of 0.82 is larger than the 0.05 value required to pass the p test[12] so that this result is highly likely. The small value for χ^2 suggests that the uncertainties may be overestimated by about ∼20%. The corresponding fit for the assumption of a constant flow longitude gives $\lambda = 75.0 \pm 0.3$ (fit 4), which has a p-value of 0.014 and is now a statistically acceptable fit, but with a lower likehood than a fit with a variable flow direction. This new fit to the data using the corrected NOZOMI uncertainties should replace the fit that is presented in Paper I.

In order to test the robustness of the fit to these data, we have performed a second fit with four additional modifications made to the input data set:

1. The uncertainties assigned to the STP 72-1, Mariner 10, and SOLRAD11B flow directions in Paper I represented the combined longitude and latitude uncertainties reported in the original publications (Section 4.3). The new fit uses only the longitude uncertainty. It is assumed that the uncertainties for longitude and latitude are normally distributed, so that the uncertainty used in Table 1 of Paper 1 can be reduced by a factor of 1.414.
2. The *IBEX* and *Ulysses* data are treated equivalently in the sense that the two independent data sets corresponding to the 2009 and 2010 seasons are included separately, rather than combined as in Paper I. The longitudes for the individual seasons from Bzowski et al. (2012) are used.

[12] As pointed out in S5 of the OSM in Paper I, the probability of taking a result χ^2 more extreme than the observed value of χ^2_{obs} is given by the p-value that equals the minimum between the two probabilities, $P(0 \leqslant \chi^2 \leqslant \chi^2_{obs})$ and $P(\chi^2_{obs} \leqslant \chi^2 \leqslant \infty)$. A null hypothesis associated with a p-value smaller than the significance level of 0.05 is typically rejected. Additional information about the statistical techniques used in the fits can be found Livadiotis (2014, 2007), Deming (1964), Lybanon (1984).

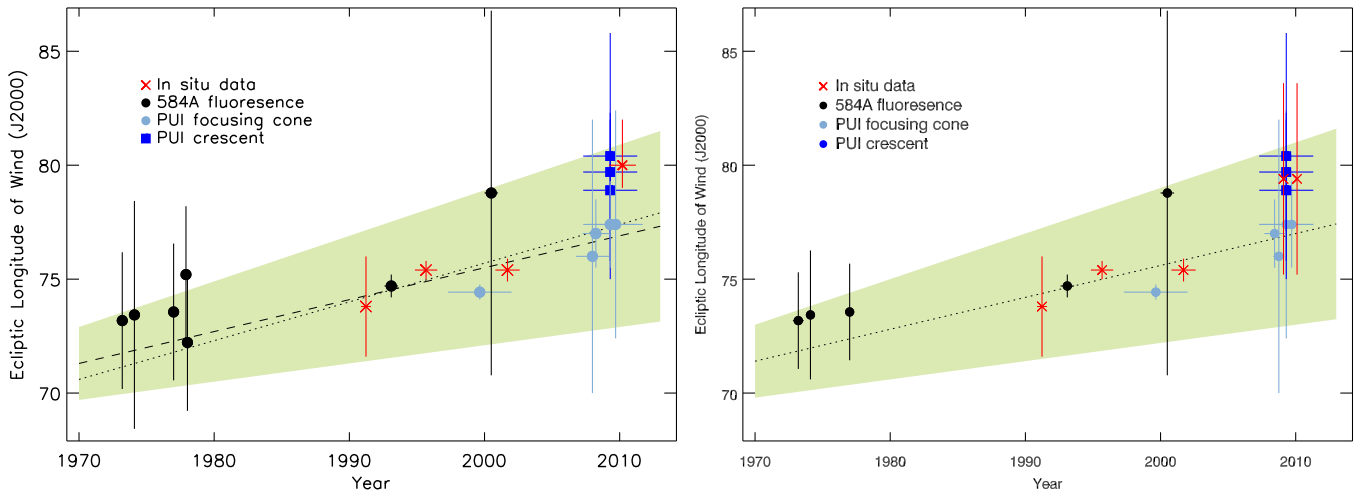

Figure 1. Left: the fit using the correct NOZOMI uncertainties is shown by the dashed line, and the dotted line shows the original (Paper I) fit with the uncorrected NOZOMI uncertainties. The shaded region shows the uncertainties for the new fit. The uncertainties on the *IBEX* data point (red dot in upper right) are constrained by the *IBEX* parameter range and the LIC temperature toward Sirius based on Fe^+, Mg^+, and Ca^+ data (Paper I, OSM-S4). Right: same fit as on the left, except that the Prognoz 6 data are omitted, the uncertainties for the STP72-1, Mariner 10, and SOLRAD11B data are revised to include only the longitude uncertainty, and seasons 2009 and 2010 of the *IBEX* data are listed as independent data points. The *IBEX* longitude in the right hand figure does not depend on any constraints that are based on temperatures obtained from LIC absorption lines. These fits are explained further in Section 3.

3. The uncertainties for the *IBEX* longitudes are based on the *IBEX* data alone, without recourse to astronomical data on the LIC. The *IBEX* temperature uncertainty range of 4400–8200 K (Section 4.1.2) can be used to set longitude uncertainties of ±4.°2 (Figure 1 of McComas et al. 2012). In Paper I a LIC temperature based on astronomical data was used, however the astronomical data reveal large variations in the LIC temperature toward different stars (Appendix A).
4. The Prognoz 6 data are omitted from this fit because both the geometric fit and the fit obtained from modeling the data are no longer considered valid by coauthors of the original papers (Section 4.3.2).

Three fits were performed on this adjusted data set, a linear fit, a fit assuming an constant flow longitude, and a parabolic fit (heading C, fits 5, 6 and 7). The goal of the fits is to test whether a temporal variation in the flow direction over time is statistically more likely than a constant flow direction over time. The linear fits listed in Table 2 are highly likely and always more likely than a fit with a constant longitude over time. The low χ^2 value of the parabolic fit suggests that the limited set of available data does not justify a second-order fit. Note that the finding that a linear fit to the data is statistically more likely than a constant or parabolic fit is not equivalent to a statement that a change in longitude must have occurred in a linear fashion.

The linear fit is statistically the most likely fit and gives a temporal variation of 5.°6 ± 2.°4 over the past 40 years (the fit is shown in Figure 1, right). This result is close to the result in Paper I. However while a constant longitude could be rejected in Paper I, the increase in the NOZOMI uncertainties makes a constant longitude over time acceptable but less likely than a variation of the longitude over time Livadiotis (2014).

The parabolic fit is included to show that a fit with a higher order polynomial yields a result that is less satisfactory than a fit with a lower order polynomial. As the order of the polynomial in the fit increases, the χ^2 should in principle decrease until it is <1 or it is $\chi^2 \sim 1$. The parabolic fit under heading C gives $\chi^2 \sim 0.6$, which tells us that the best statistical description of the temporal variation in the flow direction is given by the linear fit.

New reductions and modeling of the *Ulysses* data have appeared since the publication of Paper I (Bzowski et al. 2014; Wood et al. 2014; Katushkina et al. 2014). These results find a He^o flow longitude for the *Ulysses* data collected during the 2007 polar pass that is close to the value of Witte (2004), but with a somewhat higher temperature (7500^{+1500}_{-2000} K; Bzowski et al. 2014). The differences between the He^o flow vector found from the *IBEX* 2009–2010 seasons of data (Möbius et al. 2012; Bzowski et al. 2012; McComas et al. 2012), and the *Ulysses* vector, are not yet explained. For the latest seasons of *IBEX* observations (2012–2014; McComas et al. 2014; Leonard et al. 2014), the results from spacecraft pointings in the ecliptic suggest a different portion of the coupled four-dimensional "tube" of possible solutions presented by McComas et al. (2012) with similar He^o velocity vectors to *Ulysses* but requiring a significantly warmer cloud; other new *IBEX* pointing directions, at different angles to the ecliptic plane, are not consistent with the *Ulysses* data for reasons not fully understood. Comparisons of *Ulysses* and *IBEX* results are a study in progress and we do not include results presented after 2013 in the refitting of the data in this paper.

4. DATA USED FOR DETECTING TEMPORAL VARIATIONS IN THE NEUTRAL HELIUM WIND

LB14 have argued that most of the data incorporated into the meta-analysis of Paper I were either incorrect or were used incorrectly. These data, all of which were taken from the refereed scientific literature, fall into three groups: remote measurements of the backscattered solar 584 Å emission from interstellar He^o in the inner heliosphere (Weller & Meier 1974, 1979, 1981; Meier 1977; Broadfoot & Kumar 1978; Ajello 1978; Ajello et al. 1979; Dalaudier et al. 1984; Flynn et al. 1998; Vallerga et al. 2004; Lallement et al. 2004; Nakagawa et al. 2008, 2014); in situ measurements of the pickup-up ions that are sampled by spacecraft traversing the gravitational focusing cone and upwind crescent (Gloeckler et al. 2004; Drews et al. 2012; Gershman et al. 2013), and in situ measurements of interstellar He^o atoms (Witte 2004; Möbius et al. 2012; Bzowski et al. 2012, 2014; McComas et al. 2012).

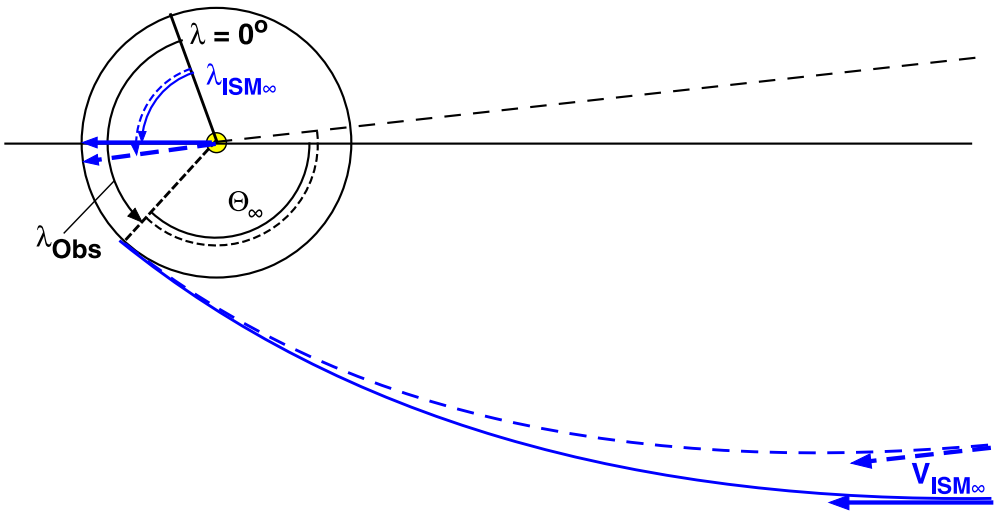

Figure 2. Hyperbolic trajectory geometry in the plane of the ISN bulk flow. The location of the perihelion (or flow tangential to the Earth's orbit) is degenerate in all combinations $V_{\rm ISM,\infty}$ ($\lambda_{\rm ISM,\infty}$) that satisfy Equation (1). The solid and the dashed blue line indicate two sample trajectories from infinity to their perihelion at $\theta = 0^\circ$ that satisfy the relation, but arrive from different inflow longitudes $\lambda_{\rm ISM,\infty}$ as indicated by the solid and dashed black lines. $\lambda_{\rm Obs}$ is the longitude of the observations, θ_∞ is true anomaly of the inflow trajectory (blue line) from infinity to perihelion at $r_{\rm E} = 1$ AU. The dashed blue line shows the trajectory of an atom with a different θ_∞–$V_{\rm ISM,\infty}$ combination that satisfies Equation (1).

Table 1 summarizes the basic LB14 arguments and our response to those arguments. Most of the arguments are speculative. The LB14 hypothesis about an underestimated *IBEX*-Lo instrument response function is wrong (Section 4.1.3, Appendix B). The better-supported argument that the *STEREO* PUI data only provide upper limits because of the azimuthal transport of PUIs inside of 1 AU has since been shown to be incorrect by the 0.1 AU parallel mean-free-path of newborn PUIs found by Gershman et al. (2014) from MESSENGER data (Section 4.2).

4.1. Evaluation of He° Flow Longitude from IBEX Measurements

4.1.1. Functional Dependencies of He° Flow Direction on Peak Neutral Fluxes

The trajectories of neutral interstellar helium atoms through the heliosphere depend on the four parameters describe the interstellar He° gas at "infinity" beyond the influence of the heliosphere, the gas flow longitude, $\lambda_{\rm ISM,\infty}$, latitude $\beta_{\rm ISM,\infty}$, speed $V_{\rm ISM,\infty}$, and temperature $T_{\rm ISM,\infty}$. In the parameter space measured by *IBEX*-Lo, these parameters are interdependent with coupled uncertainties. As discussed by Möbius et al. (2012), Lee et al. (2012) and Möbius et al. (2014), since *IBEX* is nearly a Sun-pointed spinner, the determination of the ISNs inflow vector is tied to the *IBEX*-Lo observation of the flux maximum that is in a direction that is perpendicular to the Earth–Sun line. Then, as shown in Figure 2, the observed flux maximum is directly related to the bulk flow vector at 1 AU, in the plane of the ISN bulk flow trajectory. Here $V_{\rm ISM,\infty}$ and $\lambda_{\rm ISM,\infty}$ are uniquely connected by the hyperbolic trajectory equation (Equation (1)) and the relation between the true anomaly θ_∞ (the angle between the observed velocity and the flow vector at infinity) of the trajectory, the observer location when obtaining the peak λ_P, and inflow direction $\lambda_{\rm ISM,\infty}$, so that $\theta_\infty = \lambda_{\rm ISM,\infty}+180^\circ - \lambda_P$ is

$$V_{\rm ISM,\infty} = \left[\frac{GM_{\rm S}}{r_{\rm E}}\left(\frac{-1}{\cos(\theta_\infty)} - 1\right)\right]^{1/2}. \quad (1)$$

Without further information, this constitutes a functional relationship of $V_{\rm ISM,\infty}$ ($\lambda_{\rm ISM,\infty}$). The location of the flow maximum observed by *IBEX* along the Earth orbit $\lambda_{\rm Peak}$ was determined to be $130 \pm 0.^\circ 7$ in (Möbius et al. 2012), which constrains the functional relationship in Equation (1) to within $\leqslant \pm 0.^\circ 7$ in $\lambda_{\rm ISM,\infty}$ and $\leqslant \pm 0.5$ km s^{-1} in $V_{\rm ISM,\infty}$, although a large range of values along the function satisfy the observed location of the interstellar gas flow maximum at 1 AU nearly as well.

Simultaneously, the ISN flow direction in latitude $\beta_{\rm ISM,\infty}$ ($\lambda_{\rm ISM,\infty}$) and the ISN temperature $T_{\rm ISM,\infty}$ ($\lambda_{\rm ISM,\infty}$) are determined in the Möbius et al. (2012) analysis from the ISN flow peak location in latitude and its angular width in latitude, σ_ψ, the observation of which is shown in Figure 3, again varying with the ISN flow longitude (also see Möbius et al. 2014). As indicated in the left panel of Figure 3, the observed angular distribution of the incoming interstellar neutrals constitutes a local Mach cone of width $v_{\rm Th}/V_{\rm ISM,1\,AU}$, based on the bulk flow $V_{\rm ISM,1\,AU}$ and the thermal velocity $v_{\rm Th}$ of the distribution at 1 AU. Therefore, the observed angular width fixes the ratio $T_{\rm ISM,\infty}{}^{1/2}/V_{\rm ISM,1\,AU}$, and the derived temperature depends on the derived ISN bulk flow speed $V_{\rm ISM,\infty}$, the only variable in $V_{\rm ISM,1\,AU}$, and thus on $\lambda_{\rm ISM,\infty}$. Because the statistical uncertainties of the observed peak location and width of the ISN flow are only 2% and 1%, respectively, the combined uncertainties of the two relations are mainly determined by the uncertainties in relation (1) and potential systematic effects. We will address such effects below, in particular, on the resulting temperature.

As shown in Figure 4, the latitude $\psi_{\rm Peak}$ of the flow at 1 AU in the solar rest frame is connected to the ISN flow latitude $\beta_{\rm ISM,\infty}$ at infinity through the true anomaly of the bulk flow as

$$\tan(\psi_{\rm Peak}) = \frac{\tan(\beta_{\rm ISM,\infty})}{|\sin(\theta_\infty)|} = \frac{\tan(\beta_{\rm ISM,\infty})}{|\sin(\lambda_{\rm ISM,\infty}+180^\circ-\lambda_{\rm Peak})|} \quad (2)$$

and thus again to the ISN inflow longitude $\lambda_{\rm ISM,\infty}$. These relations constitute a degeneracy in the determination of $V_{\rm ISM,\infty}$, $\beta_{\rm ISM,\infty}$, and $T_{\rm ISM,\infty}$ as a function of $\lambda_{\rm ISM,\infty}$. However, relation (2) also provides a tool to break the degeneracy using *IBEX* latitude distributions combined for different positions of *IBEX* as the observer varies in longitude $\lambda_{\rm Obs}$. Then, $\lambda_{\rm Obs}$ replaces $\lambda_{\rm Peak}$ in Equation (2) as a variable and the resulting relation $\psi(\lambda_{\rm ISM,\infty})$

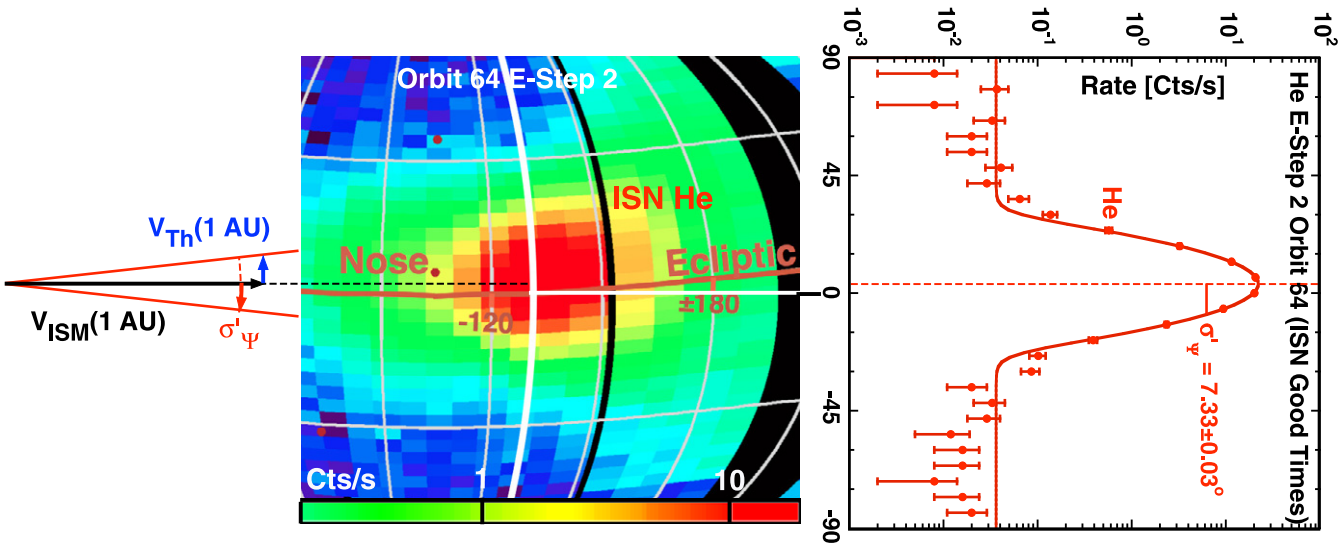

Figure 3. Composite of angular distribution measurement as a local Mach Cone, whose width (shown on the left) $\sigma'_\psi = v_{\rm th(1\,AU)}/V_{\rm ISM(1\,AU)}$ is defined by the ratio of the local thermal and bulk velocities of the flow. The angular width in latitude σ'_ψ is obtained from the cut through the maximum of the neutral helium rate distribution in ecliptic longitude (along the white arc) shown in the color coded map (center panel). The latitudinal rate distribution of that cut (right panel) is shown along with a Gaussian fit and statistical uncertainties.

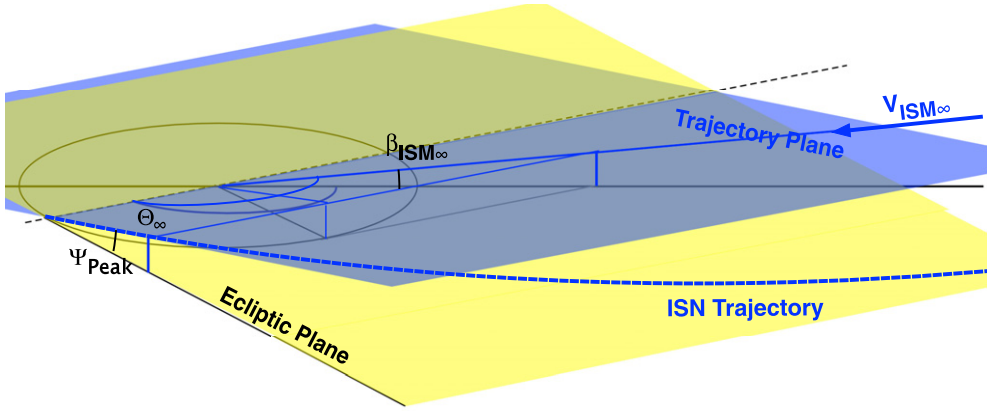

Figure 4. Schematic view of the interstellar gas flow in its trajectory plane (blue), which is inclined to the ecliptic (yellow) at the latitude inflow angle $\beta_{\rm ISM,\infty}$. $\psi_{\rm Peak}$ is the latitude of the flow in the solar rest frame, θ_∞ is the perihelion angle with respect to the interstellar flow at infinity, and $\beta_{\rm ISM,\infty}$ is the latitude of the interstellar flow at infinity. The x, y, z (and primed) coordinates define the cartesian coordinate systems.

depends distinctly on $\lambda_{\rm ISM,\infty}$. The comparison of ISN flow distributions observed over entire 2009–2010 observation seasons with the predicted relation (2) as a function of $\lambda_{\rm ISM,\infty}$ and respective χ^2-minimization in Möbius et al. (2012) resulted in the reported optimum inflow longitude $\lambda_{\rm ISM,\infty} = 79\overset{\circ}{.}0$ $(+3\overset{\circ}{.}0, -3\overset{\circ}{.}5)$ with a similar result in Bzowski et al. (2012). Bzowski et al. (2012) used a χ^2 analysis to find an uncertainty range for the interstellar flow longitude of $\sim\pm4^\circ$ (blue contour in Figure 22 of Bzowski et al. 2012). These uncertainties were the basis for the bounding values of the resulting parameter range from the *IBEX* observations used in McComas et al. (2012).

In contrast, Lallement & Bertaux (2014, in top box of Figure 2) maintain that the variation of the observed fluxes as a function of observer longitude $\lambda_{\rm Obs}$, with a substantially wider maximum than observed with *Ulysses* GAS (Witte 2004), may have led to the different inflow longitude, which may be affected by instrumental influences. To support their claim, they compare the observed *IBEX* count rate distributions with simulated distributions for the Witte (2004) parameter set produced by Bzowski et al. (2012) from the best-fitting χ^2 analysis. However, the difference in the distributions between these two sets is totally dominated by the larger angular widths of the count rate sequences measured by *IBEX*, which leads to the larger derived temperature, and not by unaccounted-for data losses. As shown by Lee et al. (2012), the widths of the distribution in latitude and longitude are tightly coupled and represent the ISN temperature.

To illustrate the basis for the inflow direction in the *IBEX* analysis, Figure 5 shows the peak location and width of the ISN flow distributions in latitude as simulated for the observation periods during the 2009 ISN season orbits. Shown are the results for two ISN flow parameters sets that lie on the center line of the parameter tube (e.g., Figure 1 in McComas et al. 2012) as defined in Equations (1) and (2), using the inflow longitude $\lambda_{\rm ISM,\infty}$ of Witte 2004 (red) and of Bzowski et al. and Möbius et al. (2012, blue). For comparison the width is shown as obtained with the temperature found by Witte (2004), which stands out as much narrower than that from *IBEX*. However,

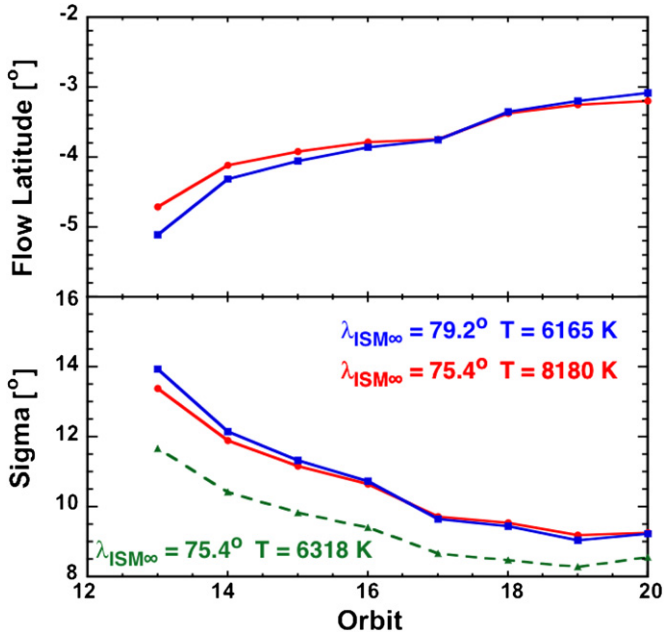

Figure 5. Peak location in latitude (top) and width (bottom) of ISN flow distributions for the *IBEX* orbits during the 2009 ISN flow season, simulated for the actual observation periods with two ISN flow parameter sets along the center of the *IBEX* tube in parameter space. The inflow longitude of Witte (2004) is shown in red and the one of Bzowski et al. (2012) and Möbius et al. (2012) in blue. The latitudinal width of the distribution, σ, is also shown in green for the temperature found by Witte (2004). These simulations are based on the measured properties of the *IBEX*-Lo instrument. A temperature of 8180 K would be required for the Witte (2004) flow vector to match the latitudinal width measured by *IBEX*.

the visible differences between the two parameter sets along the *IBEX* tube are, first, a steeper variation of the peak location as a function of orbit for $\lambda_{ISM,\infty}$ as favored by Bzowski et al. (2012) than for the value of Witte (2004) and, second, a somewhat stronger increase in width toward the early orbits. To arrive at a value for $\lambda_{ISM,\infty}$, solely the first effect has been used by Möbius et al. (2012). In relation to $\lambda_{ISM,\infty}$ the χ^2-minimization in the comparison between observed and simulated flow distributions used by Bzowski et al. (2012, see Figure 22) is sensitive to both effects as illustrated in Figure 5.

This leaves only the argument of LB14 that the width of the angular distribution, which now solely influences the derived temperature, could be brought into agreement with the *Ulysses* value by considering the influence of a strong and unaccounted-for instrumental effect in the *IBEX* data reduction. As derived from extensive tests with the actual *IBEX* data system hardware simulator and Monte Carlo simulations of realistic data throughput of a wide range of particle rates, the actual effect of data suppression due to limited transmission bandwidth on the width of the observed distributions is <2% and thus is negligible (see Appendix B, including Figure 6).

LB14 (p. 1) make the point that the degeneracy between the longitude and velocity of the He° distribution function allows the longitude of the peak count rates of *IBEX* data to also correspond to the expectations for the *Ulysses* flow vector, providing there is an additional suppression of count rates (detector "dead-time") that was neglected in the *IBEX* data flow.[13] In support of their hypothesis that the helium vector of Witte (2004) is correct, LB14 took the orbit-by-orbit *IBEX* data, and the simulations where Bzowski et al. (2012, Figure 18) compared the *IBEX* data with the *Ulysses* flow parameters. Those rates and data simulations were replotted for two cases (Figure 2 of LB14). One line on the plot showed the results of the Bzowski et al. (2012) analysis, while the other line plotted an adjusted count-rate based on the LB14 hypothesized 7 ms dead-time correction for the *IBEX*-Lo instrument. They argued that the Witte (2004) flow direction agreed with the *IBEX* count rates for their hypothesized dead-time correction.[14] This argument to reject the *IBEX* analysis because of a hypothesized 7 ms dead-time correction is not valid.

The effect that influenced the *IBEX* data flow is a known finite data processing time, not a sensor dead-time, and the types of events mostly responsible for this effect were unanticipated electrons, which do not alter the shape of the observed interstellar flow distribution significantly. Also, these are excluded by a new instrument mode that started mid-2012. This operational modification has eliminated the count rate reduction effect almost entirely. Comparison between the old and new operational modes has demonstrated that the finite data processing time does not significantly affect the count rate distributions used to reach the conclusions reported in Möbius et al. (2012), Bzowski et al. (2012), and McComas et al. (2012, Appendix B). In particular, the data processing time did not influence the deduced He temperature, which LB14 tried to reconcile by exploring this effect to an extent that was already excluded by Möbius et al. (2012). The instrument response function of *IBEX*-Lo does not contribute in any significant way to the uncertainties of the interstellar He° flow direction derived from the *IBEX* data. This is discussed in more detail in Appendix B.

In summary, the inflow longitude parameter hinges mostly on the evolution of the peak location in latitude as a function of observer longitude in the *IBEX* observations. While the temperature in Möbius et al. (2012) is obtained by fitting the height and width of the count rate distributions, these observables were ignored in LB14. The temperature derived from the *IBEX* observations, for the case where one assumes the inflow velocity of the *Ulysses* results (Witte, 2004), is 30% higher than the temperature reported from *Ulysses* GAS observations of He°. Systematic instrumental effects larger than 2% in the *IBEX* observations, such as an erroneous instrument response function, can be ruled out as the reason for the difference between the *Ulysses* and *IBEX* He° flow directions (also see Appendix B).

4.1.2. IBEX Results for 2009–2010 Seasons of Data

IBEX-Lo directly samples the trajectories of interstellar He atoms at 1 AU after they have survived photoionization, electron-impact ionization, and charge-exchange with the Solar wind to reach the 1 AU orbit of *IBEX* (McComas et al. 2009; Fuselier et al. 2009a, 2009b; Möbius et al. 2009, 2014, 2012; Bzowski et al. 2012). *IBEX*-Lo collects interstellar helium atoms over several orbits during late winter and early spring where the atoms are near perihelion of their trajectories (Lee et al. 2012). In the earliest orbits, *IBEX*-Lo samples the "warm breeze" that consists of secondary He° atoms that are deflected beyond the heliopause (Kubiak et al. 2014). After that the direct interstellar He° wind dominates the count rate.

[13] More specifically, they state that "We have examined the consequences of dead-time counting effects, and conclude that their inclusion at a realistic level is sufficient to reconcile the [*IBEX* 2009–2010] data with the *old* [Witte *Ulysses*] parameters, calling for further investigations." (LB14, p. 1)

[14] LB14 (p. 5) state: "...it is premature to use the new longitude and velocity [of *IBEX*] before the question of the dead-time correction is fully settled."

The interstellar helium wind direction was obtained from these measurements using two independent analysis methods. Möbius et al. (2012) used an analytical approach to fit the evolution of the helium count rates across the orbits where helium is observed, where the outer boundary of the computations was at infinity. Bzowski et al. (2012) compared simulations of the helium distribution obtained from the Warsaw Test Particle model with the *IBEX* data, and performed χ^2−fitting between the models and data to obtain the best helium wind parameters, where the outer boundary of the computations was at 150 AU, the distance at which the interaction is already underway. McComas et al. (2012) resolved the small discrepancy caused by the different outer boundaries used in the two computations and showed that these independent analyses of the *IBEX*-Lo data yield similar results.

Independent analysis of the 2009 and 2010 seasons of *IBEX* data yielded the same flow direction within a large acceptable range. For the *IBEX* flow direction during the 2009 observing season, Bzowski et al. (2012) found a He flow vector of $\lambda_{\rm ISM,\infty} = 79\overset{\circ}{.}2$, $\beta_{\rm ISM,\infty} = -5\overset{\circ}{.}06$, $V_{\rm ISM,\infty} = 22.831$ km s^{-1}, and $T_{\rm ISM,\infty} = 6094$ K. For the 2010 season, the He$^{\rm o}$ flow vector was $\lambda_{\rm ISM,\infty} = 79\overset{\circ}{.}2$, $\beta_{\rm ISM,\infty} = -5\overset{\circ}{.}12$, $V_{\rm ISM,\infty} = 22.710$ km s^{-1}, and $T_{\rm ISM,\infty} = 6254$ K. These solutions also provided acceptable χ^2 values for mutual fits of the four interdependent parameters (Figure 22 in Bzowski et al. 2012). The acceptable range for the longitude is $75\overset{\circ}{.}2$–$83\overset{\circ}{.}6$, corresponding to temperatures of 4400–8200 K, with each flow longitude coupled to a tightly constrained range of the other parameters because the uncertainties are correlated. In contrast, when the *Ulysses* helium flow longitude (Witte 2004) was used as a constraint to the *IBEX* longitude data, the best reduced χ^2 fit was an order-of-magnitude larger (Figure 17 in Bzowski et al. 2012). Independently, and with the analytic method described by Lee et al. (2012), Möbius et al. (2012) determined a flow vector for the combined 2009–2010 seasons of $\lambda_{\rm ISM,\infty} = 79.0^{+3.0}_{-3.5}$ deg, $\beta_{\rm ISM,\infty} = -4.9 \pm 0.2$ deg, $V_{\rm ISM,\infty} = 23.5^{+3.0}_{-2.0}$ km s^{-1}, and $T_{\rm ISM,\infty} = 6200^{+2000}_{-1200}$ K. The best-fitting direction of the interstellar helium wind using two different analysis techniques are in good agreement with each other.

The large range of possible longitudes that is obtained when the correlated uncertainties of the four-dimensional parameter are included can be constrained further if independent information on the LIC temperature is available. In Paper I we used the gas temperature that is obtained from astronomical observations of the spectra of refractory interstellar elements toward Sirius (see Appendix A).

One outcome of the Bzowski et al. (2014) reanalysis of the *Ulysses* data set is that the "suspicious" coincidence remarked upon by LB14, that the latitude of the He$^{\rm o}$ flow did not vary between the *IBEX* and *Ulysses* He$^{\rm o}$ measurements, may not be so settled after all with the new reduction and modeling of the *Ulysses* data. Bzowski et al. (2014) found that the best-fit *Ulysses* upwind direction of the flow latitude is one degree north of the center of the *IBEX* range, at $\beta_{\rm ISM,\infty} = 6^\circ \pm 1\overset{\circ}{.}0$ versus $\beta_{\rm ISM,\infty} = 4\overset{\circ}{.}98 \pm 1\overset{\circ}{.}21$ for *IBEX* (McComas et al. 2012).

4.1.3. IBEX Instrumental Response Function

In order to support their perspective that the interstellar wind direction through the heliosphere is invariant with time, LB14 speculated that the instrumental response function used to analyze the *IBEX*-Lo data is incorrect, and argued that the true "dead-time" correction is 7 ms, which is larger than the value of the instrument response function underlying the *IBEX* data analysis of the 2009–2010 observing seasons. An explanation of the incorrectness of this speculation is given in Appendix B, where the details of the *IBEX* instrumental function are discussed.

In addition, the ISN flow direction is driven by the variation of the peak in latitude with the ecliptic longitude of *IBEX*, which is not affected by data flow restrictions. *IBEX* is a Sun-pointed spinner that measures vertical swaths of the sky with each spin (McComas et al. 2009). The He$^{\rm o}$ particle trajectories are measured over both longitude and latitude, and that are insensitive to the speculations of LB14 regarding the instrumental response parameter (Section 4.1). The best-fitting ISN flow direction found from *IBEX* observations (Section 4.1.2) is not dominated by the longitudinal height and width of the observed flux distribution.

LB14 have also claimed that the second independent analysis of *IBEX* data by Bzowski et al. (2012) omits "dead-time" corrections. This argument is invalid because the Bzowski et al. results are based on data that used an instrument response function that had been tested and validated.

4.2. STEREO Measurements of Pickup Ions

Measurements of He, Ne and O PUIs by the *STEREO* PLASTIC instrument between 2007 and 2011 are reported by Drews et al. (2012, hereafter D12). Neutral interstellar He, Ne and O atoms penetrate to the inner heliosphere where they are ionized by photoionization, electron-impact ionization, or charge-exchange with the solar wind (Bzowski et al. 2013).[15] The charged particles that form inside of 1 AU couple to the solar wind magnetic field and are convected radially outward with the solar wind where they can be observed at 1 AU. Helium and Ne survive the larger ionization losses associated with close passage to the Sun and become gravitationally focused in the downwind direction. Oxygen is mainly ionized in the upwind regions. Helium, Ne and O PUIs form a region of enhanced PUI density with a crescent-like distribution in the upwind hemisphere (D12). Drews et al. determined the interstellar wind longitude independently from the He and Ne focusing cones, and the upwind He, Ne and O crescents, and obtained five independent measurements of the ecliptic longitude of the interstellar wind direction (Table 2) that were used in Paper I to evaluate the statistical likelihood that the interstellar wind direction had changed over the past forty years.

LB14 conclude that the *STEREO* PUI data are only valid as upper limits on the interstellar wind longitude, and that the oxygen data should be ignored entirely. In more detail they argue that: (1) PUI transport inside of 1 AU causes deviations of the location of the focusing cone and crescent of up to 5° so that values for the flow directions obtained from *STEREO* PUI can only be taken as upper limits. (2) The requirement of a smoothly varying ionization rate used in the *STEREO* analysis is not satisfied. They claim that D12 only consider photoionization and not considered ionization by electron impacts. (3) The intercomparison of the data between orbit groupings are invalid because the data are not statistically independent. (4) The statistical simulations of the direction uncertainties of the

[15] Photoionization models of the LIC predict neutral fractions at the heliosphere for hydrogen, helium, neon, and oxygen of ∼0.78, ∼0.61, ∼0.20, and ∼0.80 respectively (Slavin & Frisch 2008). Up to 60%, 30%, and 4% of these neutral interstellar He, Ne and O atoms, respectively, survive to the Earth's orbit before being ionized by a mix of electron-impact ionization, charge-exchange with the solar wind, and photoionization (Bzowski et al. 2013). PUI data sample particles created between the Sun and the observation point.

STEREO analysis are incorrect. (5) Oxygen should not be used to infer the interstellar flow since there is also a population of secondary oxygen atoms.

4.2.1. Transport of PUIs in the Expanding Solar Wind

PUIs are created in the turbulent environment inside of 1 AU. If the mean-free-path for transport of the newly formed PUIs is large, $\lambda_{\parallel} \sim 1$ AU, PUI ions are transported parallel to the magnetic field lines so that their spatial distribution is no longer a valid marker of the ISN wind direction (Chalov 2014).[16] However if the PUIs are formed in a non-turbulent environment, e.g., $\lambda_{\parallel} \sim 0.1$ AU, the parallel transport is negligible. A new MESSENGER study has shown that $\lambda_{\parallel} \sim 0.1$ AU in the region 0.1–0.3 AU from the Sun (Gershman et al. 2014). These new results invalidate the main argument of LB14 that the PUI data should not be used for determining the direction of the interstellar neutral wind. However, we reach this conclusion with the understanding that new modeling of the ionization of ISNs close the Sun is providing new insights into the stability of the focusing cone and crescent locations that may affect these conclusions (J. Sokol 2014, private communication).

LB14 based their conclusions regarding the PUIs on a study of Chalov & Fahr (2006), who found that transport effects could generate a relative azimuthal displacement of PUIs to positive longitudes of up to five degrees, but that the transport effect was insignificant for the range of $w = v_{\rm ion}/v_{\rm sw} > 1.4$ in the SWICS data from *ACE* because of instrumental properties. However the *STEREO* data used by D12 is for PUIs with $w > 1.5$ so the Chalov & Fahr (2006) modeling does not apply.

In addition to the new MESSENGER results, three other sets of measurements of the ISN flow longitude obtained from focusing cone measurements after 2007 agree with each other. The longitude for the He^{o} ISN flow found from *STEREO* data collected 2007–2011 is $77\overset{\circ}{.}4 \pm 1\overset{\circ}{.}9$ (Drews et al. 2012). It is consistent with the *ACE* SWICS and MESSENGER FIPS data collected over the first two years of this interval. Also, Gershman et al. (2013, G13) analyzed *ACE* SWICS 1 AU data from 2007–2009 and found a longitude $77\overset{\circ}{.}0 \pm 1\overset{\circ}{.}5$ that was consistent with the ISN flow direction, $76\overset{\circ}{.}0 \pm 6\overset{\circ}{.}0$, collected by MESSENGER at 0.3 AU during three passes through the focusing cone during 2007–2009. Gershman et al. (2013) concluded that the similar longitudes found from the 1 AU SWICS data and the 0.3 AU FIPS data indicated that azimuthal transport effects have a minimal effect on the He^{o} flow longitude, and that electron impact ionization is significant inside of 1 AU.

However, as noted above, transport effects appear to have a minimal effect on the direction of the He focusing cone. *STEREO* (Drews et al. 2012), and MESSENGER and *ACE* (Gershman et al. 2013) measurements of the helium focusing cone were collected conducted during similar temporal intervals of 2007–2009, during solar minimum, and found focusing cone directions in agreement. The MESSENGER data were collected at 0.3–0.7 AU while *ACE* and *STEREO* data were obtained near 1 AU, suggesting that transport effects are insignificant. However the larger uncertainties on the He^{o} flow longitude obtained from the MESSENGER measurements, $77\overset{\circ}{.}0 \pm 6\overset{\circ}{.}0$, do not allow possible transport effects to be ruled out conclusively. The *IBEX* 2009 in situ measurements were collected over a similar time period and agree with the PUI focusing cone longitude (Möbius et al. 2012; Bzowski et al. 2012). Comparisons between the *ACE* PUI results (Gloeckler et al. 2004) and the *Ulysses* in situ He^{o} results (Witte 2004), collected at similar times but different radial distances, identify similar helium flow directions.

Although the possible transport of PUIs inside of 1 AU remains an important question because of large uncertainties on the helium focusing cone longitude in the *STEREO* data, and because of the large electron impact ionization rate that varies with time, available data suggest that it is not significant.

4.2.2. Temporal Variations in PUI Count Rates

The geometric properties of the gravitational focusing cone and upwind crescent vary with both the solar magnetic activity cycle and the solar rotation. The PUIs observed at 1 AU are seeded by the ionization of neutrals inside of 1 AU (Bzowski et al. 2013), and subsequent outward convection as part of the solar wind with a distinct energy distribution (Vasyliunas & Siscoe 1976).

In the approach used by D12, both slowly and rapidly varying influences on the observed cone and crescent structure are included in the analysis, but due to the different origins of long-term and short-term modulations they are included in distinctly different ways. Slowly changing modulations of the PUI count rates include possible variations of the ionization rate induced by solar UV radiation or by slow decay of instrumental detection efficiency. Either would result in a systematic shift of the focusing cone and crescent location in ecliptic longitude. These shifts can go in either direction, and they depend purely on the nature of the modulation. Temporal variations in the interstellar wind direction were assumed to be negligible.

Drews et al. (2012) estimated the influences of the slowly varying count rate modulation of interstellar PUIs on the results and explicitly included those variations in the analysis. Comparisons between SWICS PUI data and the solar UV emission over a ten-year period of time showed that the influence of slowly varying ionization rates induced by solar UV radiation is negligible. Influences of a slowly decreasing detection efficiency induced by aging of the PLASTIC's microchannel plates were considered explicitly in the *STEREO* analysis by estimating the slowly varying detection efficiency decay with time. Other slowly varying modulations of the observed PUI count rates, e.g., the effect of the eccentricity of the orbit of *STEREO* around the Sun, have been thoroughly discussed in D12.

PUI count rate modulation over *short timescales*, on the other hand, are included implicitly through the statistical approach used by D12. The short-term modulations mainly stem from solar wind density compressions, changes of the solar magnetic field, or solar wind variabilities such as the electron impact ionization rates (that LB14 claim are ignored). As demonstrated in D12, the statistical approach is especially well-suited to deal with these kinds of fluctuations.

The influence of electron impact ionization at 1 AU is strongly coupled to the occurrence of dense solar wind streams (Bzowski et al. 2013) and therefore fluctuates on short time scales. LB14 argue that the statistical analysis does not include the

[16] Chalov (2014) has investigated the influence of transport effects on the helium focusing cone position for the unusual solar minimum conditions between 2007 and 2009, an interval that is included in the *STEREO* measurements. By numerically solving the transport equation of He^{+} PUIs, the possible displacement of the helium focusing cone was evaluated for different values of the mean free path of the atom parallel to the magnetic field, $\lambda_{\parallel}$. For the most extreme conditions, $\lambda_{\parallel} = 1$ AU gave an offset angle for the observed focusing cone center of 3°, which would then need to be subtracted from the measured value to get the true inflowing wind direction. However for $\lambda_{\parallel} = 0.1$ AU of the MESSENGER data, no transport is found.

modulation of PUI count rates by electron impact ionization.[17] This statement is misleading because the statistical analysis focuses specifically on using the statistics of the total data set as the basis for reliably separating out and characterizing short-term variations such as electron impact ionizations.

LB14 make contradictory arguments that the analysis of the *STEREO*/PLASTIC data influences of electron impact ionization were ignored, but also that the ISM flow direction derived from Gaussian fits to numerically co-added orbital counts, without further evaluation of the data, is more accurate. This second method is based on pure geometry and explicitly ignores all influences on the formation of PUIs including those that are caused by variations in electron impact ionizations, while the D12 statistical analysis takes those influences into account.

Further details of the analysis of the *STEREO* PUI data are discussed in Appendix C, including the separation of temporal and spatial variations in the data set, the intercomparison between the four orbits acquired over the years 2007–2011, and additional statistical tests on the *STEREO* results.

4.2.3. Effect of Secondary Populations

LB14 argue that the neutral interstellar wind (NISW) longitude that is derived from the oxygen PUIs in the upwind cresent is invalid because of the presence of secondary oxygen atoms. These atoms, however, are inconsequential for measurements of the oxygen PUIs in the upwind crescent.

The populations of secondary interstellar neutral atoms are produced by interstellar ions that enter the outer heliosheath regions, and are first offset by the Lorentz force as they migrate through the ISMF draped over the heliopause, and then become neutralized through charge-exchange or recombination so that some of them enter the heliosphere. *IBEX* may have detected the secondary populations of He and O (Möbius et al. 2009, 2012; Bzowski et al. 2012) but the interpretation is still not clear (Kubiak et al. 2014). These expected secondary populations are significantly slower than the primary He and O neutrals (Izmodenov et al. 1999), and therefore have much lower probabilities of surviving in significant numbers to the inner heliosphere compared to the primary populations (Bzowski et al. 2013). Less than 20% of the interstellar oxygen is expected to be ionized (Slavin & Frisch 2008) in the LIC, so there are relatively few atoms in the potential parent population for the secondary O. For a likely asymmetric heliosphere, secondary populations of heavy species such as oxygen will be produced away from the upwind-downwind axis, where their thermal speeds will be less than the plasma flow speed in the production region, so they are less likely to reach the 1 AU region. When the relatively few secondary oxygen atoms are coupled to the long travel times through the heliosphere for secondary populations, combined with the rapid ionization of oxygen due to photoionization and charge-exchange with solar wind protons (e.g., see Bzowski et al. 2013), secondary oxygen is highly unlikely to alter the direction of the interstellar oxygen flow through the inner heliosphere that is inferred from the O PUIs.

The crescent locations deduced from He^+, Ne^+, and O^+ PUI observations show a good agreement within the uncertainties given in D12. Because any secondary flow of neutral helium and neon is at best at insignificant levels in the analysis, influences by a secondary oxygen flow are most likely insignificant, as pointed out in D12. In addition, any effect on the O^+ crescent from a secondary component would push the structure to even higher longitudes than the one reported in D12. As Lallement et al. (2005) showed based on Lyman alpha backscatter observations, the combined inflow direction of primary and secondary hydrogen is shifted toward smaller longitudes, which would then be expected also for the combined primary and secondary oxygen population. Möbius et al. (2009) indeed mentioned a structure in the neutral interstellar O flow that may be consistent with a secondary component shifted toward the same side as reported for H by Lallement et al. (2005).

4.3. He^o 584 Å Backscattered Emission

The gravitational focusing cone was first measured in 1972 through the fluorescence of solar HeI 584 Å emission from interstellar He^o close to the Sun (Weller & Meier 1974). Since then, 40 years of measurements of the interplanetary 584 Å fluorescence form a historical record of the interstellar wind direction (Ajello 1978; Ajello et al. 1979; Weller & Meier 1981; Dalaudier et al. 1984; Vallerga et al. 2004; Nakagawa et al. 2008). The 584 Å data are the earliest measurements of the interstellar wind direction and velocity.

LB14 question the treatment of the He^o 584 Å backscattering data in Paper I for three reasons: (1) they claim that the He^o wind direction used in Paper I, and obtained from the Mariner 10 data (Ajello 1978; Ajello et al. 1979), is not based only on the He^o 584 Å emission.[18] (2) They contend that the value for the flow longitude in Dalaudier et al. (1984) that is based on Prognoz 6 measurements of the geometric center of the peak 584 Å emission from the He^o focusing cone, is inaccurate and should not be used. (3) They argue that the uncertainties used for the longitude determined from the NOZOMI 584 Å measurements (Nakagawa et al. 2008) are incorrect and larger than the value used in Paper I ($\pm 3\overset{\circ}{.}4$, that was taken from the original NOZOMI publication). After Paper I was published, an erratum for the NOZOMI measurement was published (see below), so that this argument of LB14 argument was correct. It is important to note that this increase in the NOZOMI uncertainties leads to an statistically possible constant flow longitude of $75\overset{\circ}{.}0 \pm 0\overset{\circ}{.}3$ using the same assumptions as in Paper I, albeit at a lower likehood than a flow longitude that varies linearly with time (Section 3, Table 2).

4.3.1. Mariner 10 Data:

Overlooking the discussion of the Mariner 10 data in the OSM to Paper I, LB14 claim that the longitude of the NISW used for the Mariner 10 data in Paper I is based on both He^o and H^o data. The resonant He^o 584 Å emission feature was observed during two roll control maneuvers (RCMs) of Mariner 10—RCM10 on 1974 January 28 (Ajello 1978), and RCM3 on 1973 December 8 (Ajello et al. 1979). Both the He^o 584 Å and H^o Lyα emissions were observed during RCM10. From the simultaneous modeling of the two RCM10 data sets, Ajello (1978) found the direction of the interstellar gas flow. The RCM3 observations were obtained while the spacecraft was located close to the axis of symmetry of the He^o focusing cone so that the RCM3 data gave unique and independent results for the direction of the He^o focusing cone. The RCM3 He^o wind direction agrees with the wind direction in Ajello (1978) that is based on both He^o and H^o fluorescence data. Ajello et al. (1979) state that a change in the location

[17] They comment that "Drews et al. (2012) consider only the photoionization, and omit the second source of ionization, electron impact." (LB14, p. 6)

[18] They state (p. 6): "We note, however, that the direction quoted in this work has been derived from H Lyα observations, namely from the downwind Lyα minimum, i.e., it applies to the neutral hydrogen and not to helium."

of the interstellar wind axis by more than 5° degraded the fits to the RCM3 584 Å measurements. The ±5° uncertainties in Paper I are generous since Ajello et al. (1979) quote them for the combined longitude and latitude, while in Paper I we adopted the full uncertainty for the longitude alone.

4.3.2. Prognoz 6 Data

The argument of LB14 that the geometric wind direction from the He° 584 Å backscattered emission data from Prognoz 6 should not be used is puzzling because Bertaux is a coauthor on the study (Dalaudier et al. 1984). LB14 object to our use in Paper I of the wind direction found from the geometric center of the 584 Å emission pattern, even through it was quoted with uncertainties by Dalaudier et al. (1984). The Prognoz 6 analysis was later revised in two papers in order to force agreement with results from other experiments (Chassefiere et al. 1988; Lallement et al. 2004). The meta-analysis in Paper I incorporated unbiased data published with uncertainties, so we assumed that both of the He° wind directions from Prognoz 6 were useful. However, in light of the LB14 comments and the later revisions of the Prognoz 6 results, we provide a new fit to the historical data that omits both of the Prognoz 6 data points (Section 3).

4.3.3. NOZOMI Data

In Paper I we used the longitude 258.°7 ± 3.°4 for the He° flow longitude quoted in Section 6 of Nakagawa et al. (2008). Referring to the ±3.°4 uncertainties that we used for the NOZOMI data, LB14 state that the NOZOMI article contains. . .” no justification anywhere of such an uncertainty. . .” (p. 6) and this is incorrect. However, LB14 *are* correct with their argument that the ±3.°4 uncertainty is too small. We now know that the ±3.°4 uncertainty given in the original paper was a typographical error. The NOZOMI team has most kindly provided the corrected values for the upwind direction of the He° flow: $\lambda = 258.°78 \pm 8.°0$, $\beta = 3.48 \pm 8.°0$ (Nakagawa et al. 2014). In our refit to the historical data on the He° flow direction, we have therefore adopted these corrected uncertainties for the He° flow longitude from the NOZOMI data. We note that the corrected NOZOMI longitude affects the statistical likelihood of a constant flow direction over time using the otherwise same data set as used in Paper I (Section 3).

5. CONCLUSIONS

While the LB14 speculations about the *IBEX* and *STEREO* analyses are refuted, the differences between the titles of the two papers, “On the Decades-Long Stability of the Interstellar Wind through the Solar System” for Lallement & Bertaux, versus “Decades-Long Changes of the Interstellar Wind Through Our Solar System” for Frisch et al., highlights fundamental questions about the interaction between the heliosphere and interstellar medium that are not yet understood.

It is shown that small-scale structure, $\leqslant$330 AU, in the surrounding LIC may be present. Structure over these scales is indicated by the LIC collisional mean free path, possible Alfven waves propagating along the LIC ISMF, and turbulence related to supersonic motions between the LIC and adjacent clouds that could drive shocks into the LIC.

In response to the Frisch et al. (2013) meta-analysis of available, published data at that time, where it was found that the interstellar wind direction has more likely to have changed by ∼6.°8 over the past forty years than not), Lallement & Bertaux (2014) presented a long list of arguments that supported their basis for concluding that the analysis was flawed. Chief among the incorrect speculations was that the *IBEX*-Lo instrumental response function is larger than the measured value. The suggestion that azimuthal transport of PUIs inside of 1 AU showed that PUIs can only be used as upper limits on the interstellar wind direction is contradicted by results from the MESSENGER spacecraft on PUIs inside of 1 AU. They also misunderstood the *STEREO* analysis procedure. The arguments of LB14 and our rebuttal on those arguments are summarized in Table 1.

The most valuable comment of LB14 was about the uncertainties on the NOZOMI He° wind direction, and it motivated our inquiry to the NOZOMI team about those uncertainties. A typographical error in the original publication (Nakagawa et al. 2008) has now been corrected (Nakagawa et al. 2014) and incorporated into our analysis (Section 3). A new statistical analysis that included the corrected NOZOMI uncertainty was performed on the data used in Paper I. Again, using the prior sets of observations, but including this correction, a temporal variation is statistically indicated by the data and is still statistically highly likely. However, in contrast to the findings of Paper I, the larger uncertainties of the corrected NOZOMI longitude now allow a constant flow longitude of $75.°0 \pm 0.°3$, although the likelihood of a constant flow is lower than the likelihood that the flow longitude has varied over time. The statistical fit given by header B in Table 2 should replace the fit that was provided in Paper I.[19]

The statistical fitting was repeated using improved uncertainties for the STP 72-1, Mariner 10, and SOLRAD11B results, omitting the Prognoz 6 data and using both of the 2009 and 2010 seasons of *IBEX* results. For this fit, the most likely statistical result is found from a linear fit to the temporal data. The variation over forty years corresponds to a longitude variation of $\delta\lambda = 5.°6 \pm 2.°4$. Again, a constant flow longitude over time was statistically acceptable but at a lower statistical significance than the linear variation. We emphasize that the linear fits are not equivalent to claiming that the historical variation has actually occurred as a linear shift with time.

Results from the 2012–2014 *IBEX* observing seasons of the flow of interstellar He° through the heliosphere are now being studied, however the data contains puzzling effects that suggest that more complicated processes may contribute to the interaction between interstellar He° and the heliosphere (McComas et al. 2014; Leonard et al. 2014). Those results are not included in this study.

The comparison of heliospheric data on the interstellar neutral wind over long time intervals offers the possibility of sampling small scale structure that likely exists in the surrounding interstellar material. There are now over 40 years worth of historical data on the flow of interstellar He° through the heliosphere, and not all of it has been analyzed using contemporary knowledge of the He° ionization processes. Future analyses of these historical data should enrich our understanding of the interaction between the heliosphere and interstellar medium.

This work was carried out as a part of the *IBEX* mission, funded as a part of NASA’s Explorers Program. The researchers from SRC PAS were supported by Polish National Science Center grant 2012-06-M-ST9-00455. The authors thank Harald Kurcharek for helpful discussions.

[19] This correction brings out the good side of the value of robust scientific exchanges.

APPENDIX A

LIC TEMPERATURE FROM INTERSTELLAR ABSORPTION LINES

Because of the cloudy nature of local ISM, 6%–33% of space within 10–15 pc is filled with low-density material that is identified primarily by cloud velocity (Frisch et al. 2011). Redfield & Linsky (2008) have identified an absorption component corresponding to the LIC velocity toward ~80 stars located 2.6 to 74.5 pc away. Temperatures are reported for many of these stars, including 15 stars that are within 22 pc (two of which are in a binary system). Temperatures are found from the fits to the spectral line that use an intrinsic Voight profile where the broadening is assumed to be due both to mass-dependent thermal broadening and a second mass-independent component. These temperatures are plotted in Figure 7 against the angle between the star and the LIC downwind direction. The reported temperatures range between 5200^{+1900}_{-1700} K and 12050^{+820}_{-790} K and show a tendency for the temperature to decrease toward the downwind direction. Alternatively, Redfield & Linsky (2008) also report a LIC temperature of 7500 ± 1300 K using a larger set of 19 stars out to distances of 68.8 pc. Hebrard et al. (1999) reported a LIC temperature of 8000^{+500}_{-1000} K for the binary pair Sirius A and Sirius B, from the simultaneous fitting of absorption lines from both neutrals and ions. The range of the possible LIC temperatures plotted in Figure 7 for the nearest stars indicate either that the gas temperature varies between sightlines through the LIC, or that other non-LIC clouds are at LIC-like velocities for some sightlines.

In Paper I we evaluated the LIC temperature from measurements of Fe^+, Mg^+, and Ca^+ in the LIC component toward Sirius. The analysis was restricted to these refractory species that trace both ionized and neutral gasses to avoid non-overlapping distributions of neutral and ionized species because of the ionization gradient in the LIC (Slavin & Frisch 2008). A median temperature of 5800^{+300}_{-700} K was found (see the OSM of Paper I). The temperature is consistent with the *Ulysses* temperature of Witte (2004) and the preferred He^o temperature of $T_{ISM,\infty} = 6300 \pm 390$ K found from *IBEX* data in McComas et al. (2012). This Sirius temperature was used as an independent constraint on the temperature uncertainties in the *IBEX* parameter tube, which then determined the flow longitude from the *IBEX* data that was used in the statistical analysis of Paper I. Temperatures derived from interstellar absorption lines are not used in the new fits to the data that are reported in Section 3.

APPENDIX B

THE *IBEX* INSTRUMENTAL CORRECTIONS AND RESULTS FOR THE INTERSTELLAR NEUTRAL TEMPERATURE

We have determined $T_{ISM,\infty}$ from the width of the neutral flux latitude distribution in the analytic method Möbius et al. (2012); the value obtained through χ^2-minimization by Bzowski et al. (2012) is also dominated by the latitudinal variation of the fluxes. The peak height of these distributions, and thus the width, could possibly be affected by a suppression of the data flow of individual events through the data system that depends on particle count rate. To account for such a potential effect, at that time still unknown, Möbius et al. (2012) estimated an upper limit in terms of a maximum event processing time of $\tau < 5$ ms. They modeled the suspected effect as an instrument dead-time and compared observations of the same ISN flow at *IBEX*-Lo energy steps 2 and 4, the latter with a rate lower by a factor of five and thus reduced interface traffic. Lallement & Bertaux (2014) have argued that an instrumental dead-time $\tau \approx 7$ ms would allow a reconciliation of the angular distributions observed with *Ulysses* and *IBEX*, although Möbius et al. (2012) showed that $\tau \leqslant 5$ ms is an upper limit and McComas et al. (2012) reported that the effect on the temperature is much smaller based on follow-up testing and simulation, as discussed in more detail below.

The telemetry limitation for high-flux neutral atom sources, such as the ISN flow and the Earth's magnetosphere, was anticipated, and energy-angle histograms of H and O with 6° resolution are accumulated onboard *IBEX* to normalize the reported event rates. Because the width of the *IBEX*-Lo field-of-view is already 7° FWHM and to eliminate any potentially unanticipated effects on the data flow by the limited telemetry, the angular resolution used by Bzowski et al. and Möbius et al. (2012) was restricted to 6°

The hardware interface between *IBEX*-Lo and the data handling system has a known transfer time of 1.354 ms for each individual event, which increases for the first 1° portion of each 6° bin to 2.188 ms because housekeeping data and count rates are transmitted after each event. Both transmission times are much shorter than the previously estimated maximum dead-time. In addition, the interface has a double buffer, which reduces the resulting suppression even further. The response of the interface to a large variety of event and rate combinations was tested with a hardware simulator and computed with Monte Carlo simulations. These tests and reviews of the data system hardware and software rule out response times longer than the nominal values quoted above.

It was found that the majority of the event traffic across the interface, of typical rates of 300–400 s^{-1}, originates from an unanticipated substantial electron flux through the sensor, as mentioned by Möbius et al. (2012). Electrons are identified based on their short time-of-flight and thus are completely eliminated from ENA signals. However, these events add an almost isotropic (or slowly varying) base rate that burdens the interface. Figure 6 shows simulation results for the combination of such a base rate and an angular ISN flow distribution, with a peak rate of 75 events s^{-1} (the maximum ISN event rate observed) as a function of the base event rate. Shown are the total absolute reduction factor for the base and peak event rate combination (open symbols), the reduction factor for the peak relative to the already reduced base rate (solid black), the resulting increase of the width of the angular distribution (solid red), and the increase of the deduced temperature (solid blue). While the total event flow is reduced for the observed base rates of 300–400 events s^{-1} by up to 20%, the relative reduction of the peak rate over the base is only 2.5%–3%. Only the latter reduction is relevant for any distortion of the angular distribution, and consequently the width is increased only by ~1%, which translates into an apparent increase in the deduced temperature of only 2%. Interestingly, these effects on the relative height of the peak distribution and the deduced temperature top out for a base rate of ~700 events s^{-1} at <4% for the peak rate and <2.5% for the temperature. Any systematic instrumental effects on the temperature determination from *IBEX* observations larger than 2% and on the peak fluxes as a function of longitude larger than 2.5% can be excluded for the observations analyzed thus far.

It should be noted that the type of events causing this uncertainty are the unanticipated electrons that are of very

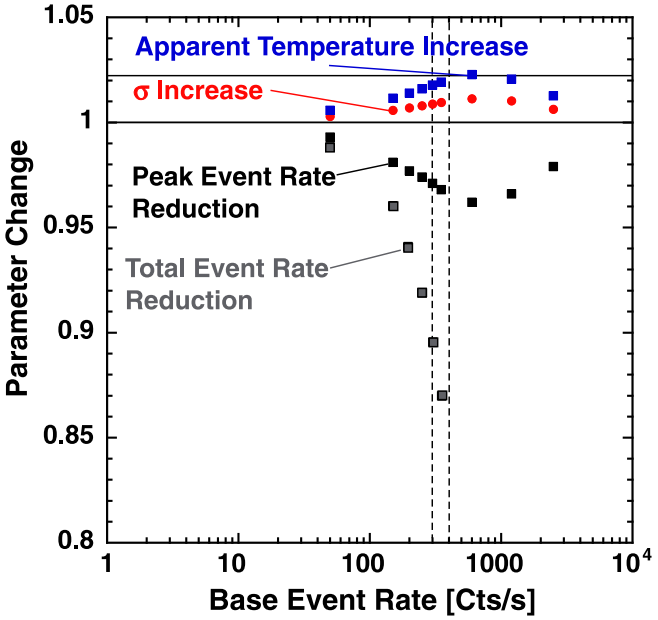

Figure 6. Simulated effects on the observed flux distribution of the ISN flow for the maximum peak rate of 75 events s^{-1}. Absolute total rate reduction (open symbols), reduction of the ISN flow peak rate relative to the base rate reduction (solid black), increase of the angular width σ in latitude (solid red), and resulting apparent temperature increase (solid blue) as a function of different continuous base event rates.

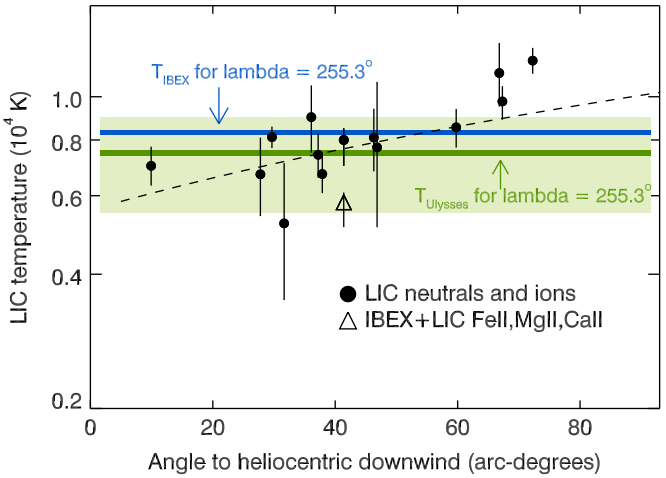

Figure 7. Temperatures of the LIC toward stars within 22 pc that sample the LIC, according to Table 1 of Redfield & Linsky (2008, dots), are plotted against the angle between the star and the ISN downwind direction ($\ell = 184°, b = -12°$ in galactic coordinates). The triangle shows the LIC temperature from Paper I, which was determined from the *IBEX* parameter range combined with Fe^+, Mg^+, and Ca^+ absorption line data in the LIC component toward Sirius. The wide green shaded region shows the uncertainty on the temperature range found from the reanalysis of the *Ulysses* data by Bzowski et al. (2014). The blue and dark-green bars show, respectively, the temperatures required by *IBEX* and *Ulysses* data if the true interstellar flow upwind direction is the best-fit value found from the *Ulysses* data, or 255°3 according to Bzowski et al. (2014). The difference between these two temperatures (853 K) shows that *IBEX* and *Ulysses* data are not in agreement. The dashed line shows a second order fit through the interstellar temperature data (dots), and is meant to guide the eye and illustrate the systematic decrease in reported cloud temperature as the angle to the downwind direction decreases. If this apparent temperature decrease is spurious, it could represent the misidentification of LIC components in sidewind directions.

little use in the *IBEX* ENA analysis, and they have been excluded by a new instrument mode that started mid-2012. This operational modification now eliminates these reduction effects almost entirely. A direct comparison of angular ISN flow distributions in both modes has verified in flight the total event rate reduction shown in Figure 5 and demonstrated that no significant broadening of the angular distribution is seen when the base event rate is present.

APPENDIX C

SEPARATING THE TEMPORAL AND SPATIAL VARIATIONS IN THE *STEREO* DATA

The analysis strategy was explained in detail in Drews et al. (2012). D12 disentangle the temporal and spatial variations in the *STEREO* data through the use of Equation (3) in their paper, where the PUI count rates are separated into the terms representing the time-independent production model for the PUIs, $V_r(\phi)$ for the azimuthal angle ϕ, and the time-dependent modulation parameter $M(t)$, which describes the fluctuations of PUI count rates induced by solar wind variabilities on short time scales. Under the assumption that the production mechanism is the same for each orbit, an approximation of the modulation parameter, $G(t)$, can be determined from the variability of the PUI count rates with respect to the average of all of the orbits, as is described through Equation (4) in their paper. The possible effects of short-term variabilities of high-speed solar wind streams or electron impact ionization were overcome by fitting the product of the time-dependent modulation parameter, $G(t)$, and a model for the angular distribution of interstellar PUIs $V_m(\phi, \lambda)$ to the angular distribution of He^+, O^+, and Ne^+ observed by *STEREO*/PLASTIC (Equation (6) in their paper). Not including $G(t)$ into the fitting procedure, i.e., $G(t) =$ constant, would mean disregarding the temporal fluctuations of PUI count rates induced by solar wind variabilities such as electron impact ionization, and is therefore comparable to a standard fitting technique, i.e., fitting a Gaussian distribution to the focusing cone and the PUI crescent.

LB14 have also objected to the method of comparing data between two separate orbits using different possible permutations of the four orbits, arguing that the different orbit combinations "are not fully independent." We disagree with this viewpoint. Due to the random nature of the PUIs fluctuations in each orbit, the intrinsic comparisons between pairs of different orbits produces independent information. The dependent variable that arises from these different permutations of orbit comparisons is the invariant component of the PUI distribution that does not change with time and depends only on the inflow direction of the interstellar helium atoms. The independent variable is the estimate of the relative modulation parameter $G(t)$, which was deduced from Equation (4) in their paper and changes for each permutation of orbit combinations. Because $G(t)$ is a key parameter to recover the inflow direction from PUI data, the intercomparison of the individual orbits is required to determine the uncertainty of the modulation parameter, $\Delta G(t)$, which in turn is necessary to determine a scientifically justified estimation of the uncertainty of the inflow direction of interstellar matter, $\Delta\lambda$.

Further simulations of the *STEREO* data are presented in Drews (2013). This extension of the statistical analysis compares two different approaches, the numerical co-adding of the count rates that ignores the time variability of the *STEREO* data, versus simulations of the properties of each orbit compared to the overall data sample. These comparisons were performed for several different sets of conditions and are presented in

Drews (2013), chapter 4.3. The statistical approach was based on 1500 randomly generated data sets using four different kind of modulations. Drews compared the results of the simulations to those of a standard fitting technique. Drews (2013, Figure 4.4) showed that the standard fitting technique provides a less precise fit to the *STEREO* data, producing an uncertainty for the focusing cone and crescent position that is ∼2 times larger than the uncertainty found using the full statistical analysis.

REFERENCES

Ajello, J. M. 1978, ApJ, 222, 1068
Ajello, J. M., Witt, N., & Blum, P. W. 1979, A&A, 73, 260
Broadfoot, A. L., & Kumar, S. 1978, ApJ, 222, 1054
Bzowski, M., Kubiak, M. A., Hlond, M., et al. 2014, A&A, 569, A8
Bzowski, M., Kubiak, M. A., Möbius, E., et al. 2012, ApJS, 198, 12
Bzowski, M., Sokół, J. M., Kubiak, M. A., & Kucharek, H. 2013, A&A, 557, A50
Chalov, S. V. 2014, MNRAS, 443, L25
Chalov, S. V., & Fahr, H. J. 2006, AstL, 32, 487
Chassefiere, E., Dalaudier, F., & Bertaux, J. L. 1988, A&A, 201, 113
Dalaudier, F., Bertaux, J. L., Kurt, V. G., & Mironova, E. N. 1984, A&A, 134, 171
Deming, W. E. 1964, Statistical Adjustment of Data (New York: Dover)
Drews, C. 2013, PhD thesis, Christian-Albreehts-Universiat zu Kiel
Drews, C., Berger, L., Wimmer-Schweingruber, R. F., et al. 2012, JGRA, 117, 9106
Flynn, B., Vallerga, J., Dalaudier, F., & Gladstone, G. R. 1998, JGR, 103, 6483
Frisch, P. C. 1994, Sci, 265, 1423
Frisch, P. C., Bzowski, M., Grün, E., et al. 2009, SSRv, 146, 235
Frisch, P. C., Bzowski, M., Livadiotis, G., et al. 2013, Sci, 341, 1080
Frisch, P. C., Grodnicki, L., & Welty, D. E. 2002, ApJ, 574, 834
Frisch, P. C., & Mueller, H.-R. 2011, SSRv, 176, 21
Frisch, P. C., Redfield, S., & Slavin, J. 2011, ARA&A, 49, 237
Frisch, P. C., & Schwadron, N. A. 2014, in ASP Conf. Ser. 484, Outstanding Problems in Heliophysics: From Coronal Heating to the Edge of the Heliosphere, ed. Q. Hu & G. P. Zank (San Francisco, CA: ASP), 42
Frisch, P. C., & York, D. G. 1991, in Extreme Ultraviolet Astronomy, ed. R. F. Malina & S. C. Bowyer (Tarrytown, NY: Pergamon), 322
Frisch, P. C. e. a., Berdyugin, A., Piirola, V., et al. 2014, Proc. 13th Annual International Astrophysics Conference, Voyager, IBEX and the Interstellar Medium, in press
Funsten, H. O., DeMajistre, R., Frisch, P. C., et al. 2013, ApJ, 776, 30
Fuselier, S. A., Allegrini, F., Funsten, H. O., et al. 2009a, Sci, 326, 962
Fuselier, S. A., Bochsler, P., Chornay, D., et al. 2009b, SSRv, 146, 117
Gershman, D. J., Fisk, L. A., Gloeckler, G., et al. 2014, ApJ, 788, 124
Gershman, D. J., Gloeckler, G., Gilbert, J. A., et al. 2013, JGRA, 118, 1389
Gloeckler, G., Möbius, E., Geiss, J., et al. 2004, A&A, 426, 845
Grogan, K., Dermott, S. F., & Gustafson, B. A. S. 1996, ApJ, 472, 812
Grzedzielski, S., & Lallement, R. 1996, SSRv, 78, 247
Hebrard, G., Mallouris, C., Ferlet, R., et al. 1999, A&A, 350, 643
Izmodenov, V. V., Lallement, R., & Geiss, J. 1999, A&A, 344, 317
Katushkina, O. A., Izmodenov, V. V., Wood, B. E., & McMullin, D. R. 2014, ApJ, 789, 80
Kubiak, M. A., Bzowski, M., Sokol, J. M., et al. 2014, ApJS, 213, 29
Lallement, R., & Bertaux, J.-L. 2014, A&A, 565, A41
Lallement, R., Ferlet, R., Lagrange, A. M., Lemoine, M., & Vidal-Madjar, A. 1995, A&A, 304, 461
Lallement, R., Quémerais, E., Bertaux, J. L., et al. 2005, Sci, 307, 1447
Lallement, R., Quémerais, E., Koutroumpa, D., et al. 2010, in Twelfth International Solar Wind Conference, Vol. 1216, 555
Lallement, R., Raymond, J. C., Vallerga, J., et al. 2004, A&A, 426, 875
Landgraf, M. 2000, JGR, 105, 10303
Lee, M. A., Kucharek, H., Möbius, E., et al. 2012, ApJS, 198, 10
Leonard, T. W., Möbius, E., Bzowski, M., et al. 2014, ApJ, submitted
Livadiotis, G. 2007, PhyA, 375, 518
Livadiotis, G. 2014, J. Stat. Distr. Appl., 1, 4
Lybanon, M. 1984, AmJPh, 52, 22
McComas, D. J., Alexashov, D., Bzowski, M., et al. 2012, Sci, 336, 1291
McComas, D. J., Allegrini, F., Bochsler, P., et al. 2009, Sci, 326, 959
McComas, D. J., Bzowski, M., Frisch, P. C., et al. 2014, ApJ, in press
Meier, R. R. 1977, A&A, 55, 211
Möbius, E., Bochsler, P., Bzowski, M., et al. 2009, Sci, 326, 969
Möbius, E., Bochsler, P., Bzowski, M., et al. 2012, ApJS, 198, 11
Möbius, E., Bzowski, M., Chalov, S., et al. 2004, A&A, 426, 897
Möbius, E., Bzowski, M., Fuselier, S. A., et al. 2014, in Proc. 13th Annual International Astrophysics Conference, Voyager, IBEX, and the Interstellar Medium, ed. G. P. Zank, in press
Nakagawa, H., Bzowski, M., Yamazaki, A., et al. 2008, A&A, 491, 29
Nakagawa, H., Bzowski, M., Yamazaki, A., et al. 2014, A&A, 566, C1
Redfield, S., & Linsky, J. L. 2008, ApJ, 673, 283
Ripken, H. W., & Fahr, H. J. 1983, A&A, 122, 181
Rucinski, D., & Bzowski, M. 1996, SSRv, 78, 265
Saul, L., Bzowski, M., Fuselier, S., et al. 2013, ApJ, 767, 130
Schwadron, N. A., Allegrini, F., Bzowski, M., et al. 2011, ApJ, 731, 56
Slavin, J. D., & Frisch, P. C. 2008, A&A, 491, 53
Slavin, J. D., Frisch, P. C., Müller, H.-R., et al. 2012, ApJ, 760, 46
Spangler, S. R., Savage, A. H., & Redfield, S. 2011, in AIP Conf. Proc. 1366, Partially Ionized Plasmas throughout the Cosmos, ed. V. Florinski, J. Heerikhuisen, G. P. Zank, & D. L. Gallagher (Melville, NY: AIP), 97
Sterken, V. J., Altobelli, N., Kempf, S., et al. 2012, A&A, 538, A102
Strub, P., Krüger, H., Sterken, V. J., & Grün, E. 2014, ApJ, submitted
Vallerga, J., Lallement, R., Lemoine, M., Dalaudier, F., & McMullin, D. 2004, A&A, 426, 855
Vasyliunas, V. M., & Siscoe, G. L. 1976, JGR, 81, 1247
Weller, C. S., & Meier, R. R. 1974, ApJ, 193, 471
Weller, C. S., & Meier, R. R. 1979, ApJ, 227, 816
Weller, C. S., & Meier, R. R. 1981, ApJ, 246, 386
Witte, M. 2004, A&A, 426, 835
Wood, B. E., Linsky, J. L., & Zank, G. P. 2000, ApJ, 537, 304
Wood, B. E., Mueller, H. R., & Witte, M. 2014, ApJ, in press